

Rapidity Spectra of Heavy Baryons in Nuclear Collisions at Various Energies : A Systematic Approach

Goutam Sau^{1*}, P. Guptaroy^{2†}, A. C. Das Ghosh^{3‡} & S. Bhattacharyya^{4§}

¹ Beramara RamChandrapur High School,
South 24-Pgs, 743609(WB), India.

² Department of Physics, Raghunathpur College,
P.O.: Raghunathpur 723133, Dist.: Purulia(WB), India.

³ Department of Microbiology,
Surendranath College, Kolkata-700009, India.

⁴ Physics and Applied Mathematics Unit(PAMU),
Indian Statistical Institute, Kolkata - 700108, India.

Abstract

This study aims at understanding the nature of measured data on the rapidity spectra of some heavy baryons [Λ , Λ bar, Ξ^- & Ξ bar $^+$] produced in the nuclear collisions at some modestly high energies. Furthermore, our objective is also to build up a comprehensive and consistent methodology to analyze the data on this specific observable which has a very important place in the domain of High Energy Physics (HEP). On an overall basis, our target here attains a moderate degree of success even for production of such rare secondaries. In addition to this, the limitations of such an approach have also been pointed out.

Keywords: Relativistic heavy ion collisions; inclusive cross-section.

PACS nos.:25.75.-q, 13.60.Hb

*e-mail: sau-goutam@yahoo.com

†e-mail: gpradeepta@rediffmail.com

‡e-mail: dasghosh@yahoo.co.in

§e-mail: bsubrata@www.isical.ac.in (Communicating Author).

1 Introduction

Production of heavy baryons in both high-energy proton-proton and nuclear collisions is relatively quite low, in so far as the qualitative aspects pertaining to the number-density and production-cross section are concerned. So, these heavy baryons are, in general, not studied very frequently in a model-based manner, though their production is physically no less significant than all other secondaries. Rather they are of great importance due to their high mass content and some other specific quantum numbers. Of them some have ‘strangeness’, for which they assume somewhat special status. In this paper we would concentrate on the studies of rapidity spectra alone on production of Λ , Λ bar, Ξ^- and Ξ bar $^+$ particle production in Pb+Pb and some other nuclear collisions at various (high) energies.

For over the last few years we had tried to build up an approach and an alternative methodology to study the rapidity spectra of the produced secondaries (both light and heavy) and succeeded to a considerable extent. And now we make new strides vis-a-vis the studies of the rapidity spectra here on production of some strange heavies in a few Heavy Ion Collisions. In the next section (Section 2) we give the outline of the approach and the methodology. The results are delivered in Figures and Tables in the Section 3. And finally, we present the conclusions in the last section (Section 4).

2 The Phenomenological Setting : General Outlook and the Method

Following Faessler[1], Peitzmann[2], Schmidt and Schukraft[3] and finally Thomé et al[4], we [5, 6] had formulated in the past a final working expression for rapidity distributions in proton-proton collisions at ISR (Intersecting Storage Rings) ranges of energy-values by the following three-parameter parametrization, viz,

$$\frac{1}{\sigma} \frac{d\sigma}{dy} = C_1 (1 + \exp \frac{y - y_0}{\Delta})^{-1} \quad (1)$$

where C_1 is a normalization constant and y_0 , Δ are two parameters. The choice of the above form made by Thomé et al[4] was intended to describe conveniently the central plateau and the fall-off in the fragmentation region by means of the parameters y_0 and Δ respectively. Besides, this was based on the concept of both limiting fragmentation and the Feynman Scaling hypothesis. For all five energies in PP collisions the value of Δ was obtained to be ~ 0.55 for pions[5] and kaons[6], ~ 0.35 for protons/antiprotons[6], and ~ 0.70 for Λ/Λ bar and Ξ^-/Ξ bar $^+$. And these values of Δ

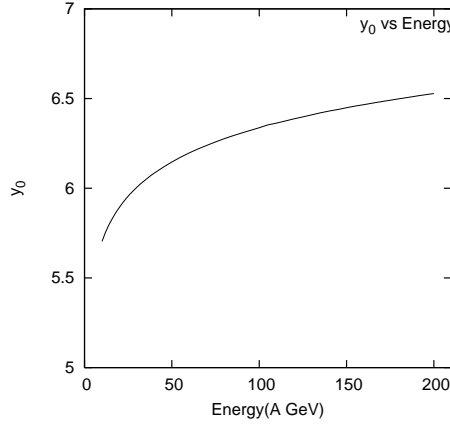


Figure 1: Variation of y_0 in equation (2) with increasing energy.[Parameter values are shown in Table 1.]

are generally assumed to remain the same in the ISR ranges of energy. Still, for very high energies, and for direct fragmentation processes which are quite feasible in very high energy heavy nucleus-nucleus collisions, such parameter values do change somewhat prominently, though in most cases with marginal high energies, we have treated them as nearly constant.

Now, the fits for the rapidity (pseudorapidity) spectra for non-pion secondaries produced in the PP reactions at various energies are phenomenologically obtained by De and Bhattacharyya[6] through the making of suitable choices of C_1 and y_0 . It is observed that for most of the secondaries the values of y_0 do not remain exactly constant and show up some degree of species-dependence . However, for lamdas (Λ , Λ bar) and cascades (Ξ^- , Ξ bar $^+$) it gradually increases with energies and the energy-dependence of y_0 is empirically proposed to be expressed by the following relationship[5]
:

$$y_0 = k \ln \sqrt{s_{NN}} + 0.8 \quad (2)$$

The nature of energy-dependence of y_0 is shown in the adjoining figure (Fig.1). Admittedly, as k is assumed to vary very slowly with c. m. energy, the parameter y_0 is not exactly linearly correlated to $\ln \sqrt{s_{NN}}$, especially in the relatively low energy region. And this is clearly manifested in Fig.1. This variation with energy in k -values is introduced in order to accommodate and describe the symmetry in the plots on the rapidity spectra around mid-rapidity. This is just phenomenologically observed by us, though we cannot readily provide any physical justification for such perception and/or

observation. And the energy-dependence of y_0 is studied here just for gaining insights in their nature and for purposes of extrapolation to the various higher energies (in the centre of mass frame, $\sqrt{s_{NN}}$) for several nucleon-nucleon, nucleon-nucleus and nucleus-nucleus collisions. The specific energy (in the c.m. system, $\sqrt{s_{NN}}$) for every nucleon-nucleus or nucleus-nucleus collision is first worked out by converting the laboratory energy value(s) in the required c.m. frame energy value(s). Thereafter the value of y_0 to be used for computations of inclusive cross-sections of nucleon-nucleon collisions at particular energies of interactions is extracted from Eq. (2) for corresponding obtained energies. This procedural step is followed for calculating the rapidity (pseudorapidity)-spectra for not only the pions produced in nucleon-nucleus and nucleus-nucleus collisions[5]. However, for the studies on the rapidity-spectra of the non-pion secondaries produced in the same reactions one does always neither have the opportunity to take recourse to such a systematic step, nor could they actually resort to this rigorous procedure, due to the lack of necessary and systematic data on them.

Our next step is to explore the nature of $f(y)$ which is envisaged to be given generally by a polynomial form noted below :

$$f(y) = \alpha + \beta y + \gamma y^2, \quad (3)$$

where α , β and γ are the coefficients to be chosen separately for each AB collisions (and also for AA collisions when the projectile and the target are same). Besides, some other points are to be made here. The suggested choice of form in expression (3) is not altogether fortuitous. In fact, we got the clue from one of the previous work by one of the authors (SB)[7] here pertaining to the studies on the behavior of the EMC effect related to the lepto-nuclear collisions. In the recent past Hwa et al[8] also made use of this sort of relation in a somewhat different context. Now let us revert to our original discussion and to the final working formula for $\frac{dN}{dy}$ in various AB (or AA) collisions given by the following relation :

$$\frac{dN}{dy}|_{AB \rightarrow QX} = C_2(AB)^{\alpha + \beta y + \gamma y^2} \frac{dN}{dy}|_{PP \rightarrow QX} = C_3(AB)^{\beta y + \gamma y^2} (1 + \exp \frac{y - y_0}{\Delta})^{-1}, \quad (4)$$

where C_2 is the normalization constant and $C_3 = C_2(AB)^\alpha$ is another constant as α is also a constant for a specific collision at a specific energy. The parameter values for different nucleus-nucleus collisions are given in the Tables (Table2 - Table 10).

3 Results

3.1 A Few Pointed Steps

The procedural steps for arriving at the results could be summed up as follows :

(i) We assume that the inclusive cross section (I.C.) of any particle in a nucleus-nucleus (AB) collision can be obtained from the production of the same in nucleon-nucleon collisions by multiplying the inclusive cross-section (I.C.) by a product of the atomic numbers of each of the colliding nuclei raised to a particular function, which is initially unspecified[9].

(ii) Secondly, we accept the property of factorization[9] of that particular function which helps us to perform the integral over p_T in a relatively simpler manner.

(iii) Thirdly, we assume a particular 3-parameter form for the pp cross section with the parameters C_1 , y_0 and Δ .

(iv) Finally, we accept the ansatz that the function $f(y)$ can be modeled by a quadratic function with the parameters α , β and γ .

3.2 Final Results Vis-a-vis the Measured Data-Sets

The results are shown here by the graphical plots with the accompanying tables for the parameter values. Here we draw the rapidity-density of Λ , Λ_{bar} , Ξ^- and Ξ_{bar}^+ for symmetric Pb+Pb, C+C and Si+Si collisions at several energies which have been appropriately labeled at the top right corner. In this context some comments are in order. Though the figures represents the case for production of Λ , Λ_{bar} , Ξ^- and Ξ_{bar}^+ , we do not anticipate and/or expect any strong charge-dependence of the results. Besides, the solid curves in all cases-almost without any exception-demonstrate our GSM-based results. Secondly, the data on rapidity-spectra for some high-energy collisions are, at times, available for both positive and negative y -values. This gives rise to a problem in our method. It is evident here in this work that we are concerned with only symmetric collisions wherein the colliding nuclei must be identical. But in our expression (4) the coefficient β multiplies a term which is proportional to y and so is not symmetric under $y \rightarrow (-y)$. In order to overcome this difficulty we would introduce here $\beta=0$ for all the graphical plots. These plots are represented by Fig.2 to Fig.14 for Λ , Λ_{bar} , Ξ^- and Ξ_{bar}^+ in Pb+Pb, C+C and Si+Si collisions under different conditions of relatively low c.m. energy values. The parameter values in this particular case are presented in Tables (Table 2 - Table 10). The graphical plots shown in Fig.2 - Fig.4 and Fig.7 (for

$\beta=0$) are for production of Λ and Λ bar in Pb+Pb interactions at 20A GeV, 30A GeV, 40A GeV, 80A GeV and 158A GeV respectively. And the plots depicted in Fig.5, Fig.6, Fig.8 and Fig.9 are based on the data on production of Λ and Λ bar in Pb+Pb collision for the five different centrality bins (for $\beta=0$) at 40A GeV and 158A GeV respectively. The diagrams shown in Fig.10, Fig.11 and Fig.12 represent the production of Ξ^- and Ξ bar $^+$ in Pb+Pb collision at 20A GeV, 30A GeV, 40A GeV, 80A GeV and 158A GeV respectively. And the diagrams in Fig.13 and Fig.14 represent the production of Λ and Λ bar in C+C and Si+Si collisions at 158A GeV.

4 Concluding Remarks

The secondaries under study here are some heaviest of the heavy secondaries on which measured data are quite sparse. Besides, the errors/uncertainties [statistical plus systematic] in the measurements of the data-sets are also quite considerable. In our work we have reckoned with only the statistical errors alone and not the systematic uncertainties, whereas the works by Alt et al and Anticic et al have attached great importance to the systematic uncertainties. Such differences in preference would make the comparison of the obtained final results a bit difficult. From the phenomenological points of view, the works by Alt et al and Anticic et al are not much different, both of whom applied the sum of two Gaussians placed symmetrically around mid-rapidity. However, the present work makes use of a form which is not purely Gaussian and has a clear but complex mass-number dependence of the nuclei in the rapidity spectra. Still, the agreements between the measured data and our model-based results are modestly satisfactory for both Λ , Λ bar, Ξ^- and Ξ bar $^+$ produced in nearly all nuclear collisions. In contrast to the observations made by both Alt et al and Anticic et al, we fail to obtain any clear rapidity-plateau at even somewhat higher energies, though the trends of the data-points have been faithfully reproduced by our approach. The neglect of the systematic uncertainties in our approach might play a crucial role in explaining this observed difference between the nature of the rapidity spectra plotted by us and those plotted by the sets of authors of Ref.[10] and Ref.[11]. Secondly, a comment is in order here with regard to the Fig.13a and 14a. We really fail to understand and account for the nature of inversion of the rapidity-spectra in these two figures related to the Λ -production in both C+C and Si+Si interactions at 158A GeV. This remains a puzzle to us, as it does not conform to the nature of all other plots, as depicted by the measured data or the model-based ones. However, a common limitation of all the approaches is

that those cannot be applied for the non-symmetric collisions in a straightforward manner. So, even the present approach cannot be considered to be a fully generalized one. Despite this, it certainly seems to provide a systematic approach to the studies on, at least, all the symmetric collisions with a complex form of nuclear mass-number dependence.

Acknowledgement

The authors express their thankful gratitude to the learned Referee for his/her constructive comments and valuable suggestions in improving the quality of an earlier version of the manuscript.

References

- [1] M.A.Faessler : Phys. Rep. **115**, 1 (1984).
- [2] T.Peitzmann : Phys. Lett. **B 450**, 7 (1999).
- [3] H.R.Schmidt and J.Schukraft : J. Phys. **G 19**, 1705 (1993).
- [4] W.Thomé et al : Nucl. Phys. **B 129**, 365 (1977).
- [5] B.De, S.Bhattacharyya and P.Guptaroy : Int. J. Mod. Phys. **A 17**, 4615 (2002).
- [6] B.De and S.Bhattacharyya : Int. J. Mod.Phys. **A 19**, 2313 (2004).
- [7] S.Bhattacharyya : Lett. Nuovo Cimento **44**, 119 (1985).
- [8] R.C.Hwa et al : Phys. Rev. **C 64**, 054611 (2001).
- [9] Goutam Sau, S.K.Biswas, A.C.Das Ghosh, A.Bhattacharya and S.Bhattacharyya : Il Nuovo Cimento **B 125(7)**, 833 (2010).
- [10] C. Alt et al (NA49 Collaboration) : Phys. Rev. **C 78**, 034918 (2008).
- [11] T. Anticic et al (NA49 Collaboration) : Phys. Rev. **C 80**, 034906 (2009).

Table 1: Variation of y_0 with Energy.[Reference Fig. No.1]

$Energy(AGeV)$	$\sqrt{s_{NN}}(GeV)$	$Constant(k)$	y_0
20	6.3	2.76	5.894
30	7.6	2.54	6.006
40	8.7	2.40	6.085
80	12.3	2.16	6.276
158	17.3	1.97	6.463

Table 2: Values of different parameters for production of Λ and Λ bar in Pb+Pb collisions at 20A GeV, 30A GeV, 40A GeV(for $\beta = 0$) for both +ve and -ve rapidities.[Reference Fig. No.2-4]

$Energy(AGeV)$	$Production$	C_3	γ	$\frac{\chi^2}{ndf}$
20	Λ	14.169 ± 0.0734	-0.073 ± 0.0012	9.075/05
20	Λ bar	0.094 ± 0.0015	-0.143 ± 0.0071	0.159/03
30	Λ	15.534 ± 0.0522	-0.049 ± 0.0004	5.288/06
30	Λ bar	0.216 ± 0.0044	-0.104 ± 0.0048	4.517/05
40	Λ	14.913 ± 0.0642	-0.035 ± 0.0005	7.540/05
40	Λ bar	0.325 ± 0.0049	-0.090 ± 0.0031	5.169/06

Table 3: Values of different parameters for production of Λ in Pb+Pb collisions at 40A GeV(for $\beta = 0$) for the 5 different centrality bins C0-C4 for both +ve and -ve rapidities.[Reference Fig. No.5]

$Centrality$	C_3	γ	$\frac{\chi^2}{ndf}$
C0	15.638 ± 0.0626	-0.039 ± 0.0004	3.644/07
C1	12.954 ± 0.0410	-0.039 ± 0.0007	1.003/07
C2	8.445 ± 0.0407	-0.037 ± 0.0005	1.922/03
C3	5.409 ± 0.0201	-0.026 ± 0.0005	0.884/03
C4	3.195 ± 0.0261	-0.026 ± 0.0009	3.662/06

Table 4: Values of different parameters for production of Λ bar in Pb+Pb collisions at 40A GeV(for $\beta = 0$) for the 5 different centrality bins C0-C4 for both +ve and -ve rapidities.[Reference Fig. No.6]

$Centrality$	C_3	γ	$\frac{\chi^2}{ndf}$
C0	0.297 ± 0.0086	-0.076 ± 0.0066	1.316/11
C1	0.234 ± 0.0074	-0.090 ± 0.0086	2.429/11
C2	0.184 ± 0.0066	-0.108 ± 0.0124	3.059/07
C3	0.147 ± 0.0029	-0.069 ± 0.0052	1.871/09
C4	0.094 ± 0.0024	-0.057 ± 0.0048	0.307/04

Table 5: Values of different parameters for production of Λ and Λ bar in Pb+Pb collisions at 80A GeV, 158A GeV(for $\beta = 0$) for both +ve and -ve rapidities.[Reference Fig. No.7]

$Energy(AGeV)$	$Production$	C_3	γ	$\frac{\chi^2}{ndf}$
80	Λ	13.841 ± 0.0254	-0.013 ± 0.0001	0.572/03
80	Λ bar	0.771 ± 0.0127	-0.025 ± 0.0031	0.946/05
158	Λ	9.473 ± 0.0317	-0.006 ± 0.0003	1.829/04
158	Λ bar	1.252 ± 0.0069	-0.049 ± 0.0008	7.249/05

Table 6: Values of different parameters for production of Λ in Pb+Pb collisions at 158A GeV(for $\beta = 0$) for the 5 different centrality bins C0-C4 for both +ve and -ve rapidities.[Reference Fig. No.8]

Centrality	C_3	γ	$\frac{\chi^2}{ndf}$
C0	13.053 ± 0.0598	-0.010 ± 0.0006	0.417/09
C1	10.779 ± 0.0318	-0.010 ± 0.0014	0.039/03
C2	8.296 ± 0.0549	-0.019 ± 0.0005	7.119/04
C3	4.760 ± 0.0085	-0.012 ± 0.0003	0.119/03
C4	3.269 ± 0.0216	-0.021 ± 0.0004	0.288/02

Table 7: Values of different parameters for production of Λ bar in Pb+Pb collisions at 158A GeV(for $\beta = 0$) for the 5 different centrality bins C0-C4 for both +ve and -ve rapidities.[Reference Fig. No.9]

Centrality	C_3	γ	$\frac{\chi^2}{ndf}$
C0	1.482 ± 0.0420	-0.049 ± 0.0032	1.912/11
C1	0.969 ± 0.0123	-0.012 ± 0.0016	0.253/05
C2	0.775 ± 0.0071	-0.021 ± 0.0015	0.252/08
C3	0.563 ± 0.0175	-0.064 ± 0.0021	1.490/05
C4	0.380 ± 0.0041	-0.065 ± 0.0049	1.388/05

Table 8: Values of different parameters for production of Ξ^- and Ξ bar $^+$ in Pb+Pb collisions at 20A GeV, 30A GeV, 40A GeV(for $\beta = 0$) for both +ve and -ve rapidities.[Reference Fig. No.10 & 11]

Energy(AGeV)	Production	C_3	γ	$\frac{\chi^2}{ndf}$
20	Ξ^-	0.961 ± 0.0073	-0.089 ± 0.0072	1.808/05
20	Ξ bar $^+$	\times	\times	\times
30	Ξ^-	1.213 ± 0.0269	-0.074 ± 0.0053	3.338/09
30	Ξ bar $^+$	0.308 ± 0.0051	-0.090 ± 0.0029	0.509/03
40	Ξ^-	1.217 ± 0.0373	-0.049 ± 0.0035	0.922/05
40	Ξ bar $^+$	0.392 ± 0.0105	-0.136 ± 0.0046	1.019/03

Table 9: Values of different parameters for production of Ξ^- and Ξ bar $^+$ in Pb+Pb collisions at 80A GeV, 158A GeV(for $\beta = 0$) for both +ve and -ve rapidities.[Reference Fig. No.12]

Energy(AGeV)	Production	C_3	γ	$\frac{\chi^2}{ndf}$
80	Ξ^-	1.577 ± 0.0335	-0.036 ± 0.0030	0.672/05
80	Ξ bar $^+$	1.538 ± 0.0444	-0.130 ± 0.0064	0.490/04
158	Ξ^-	1.491 ± 0.0268	-0.030 ± 0.0031	1.748/06
158	Ξ bar $^+$	1.604 ± 0.0336	-0.070 ± 0.0031	0.621/05

Table 10: Values of different parameters for production of Λ and Λ bar in C+C and Si+Si collisions at 158A GeV(for $\beta = 0$) for both +ve and -ve rapidities.[Reference Fig. No.13 & 14]

Collision	Production	C_3	γ	$\frac{\chi^2}{ndf}$
C + C	Λ	0.240 ± 0.0027	0.033 ± 0.0051	1.265/05
C + C	Λ bar	0.066 ± 0.0001	-0.075 ± 0.0015	0.586/07
Si + Si	Λ	0.841 ± 0.0029	0.019 ± 0.0013	4.757/07
Si + Si	Λ bar	0.163 ± 0.0014	-0.054 ± 0.0031	0.997/09

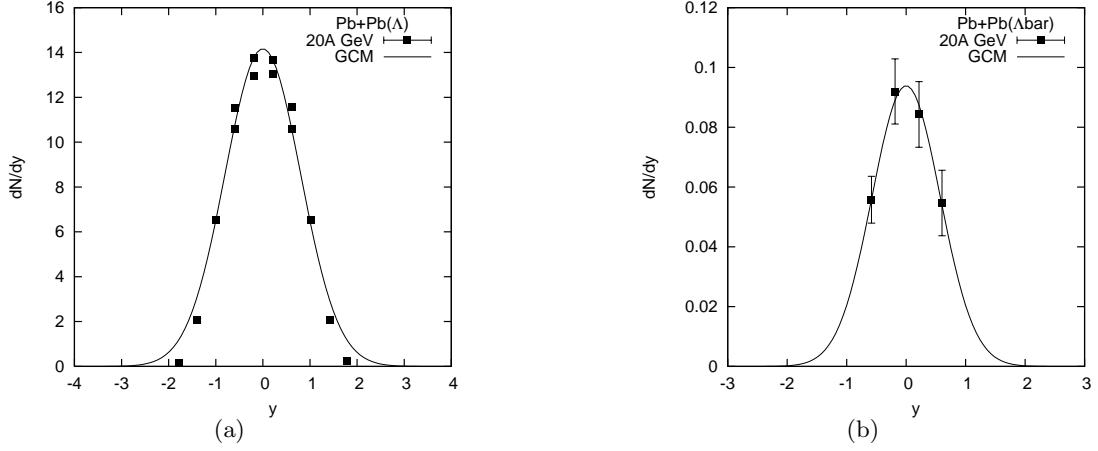


Figure 2: Plot of $\frac{dN}{dy}$ vs. y for Λ and $\Lambda\bar{\Lambda}$ produced in Pb+Pb collisions at 20A GeV for $\beta=0$. The different experimental points are taken from [10] and the parameter values are taken from Table 2. The solid curve provide the GCM-based results.

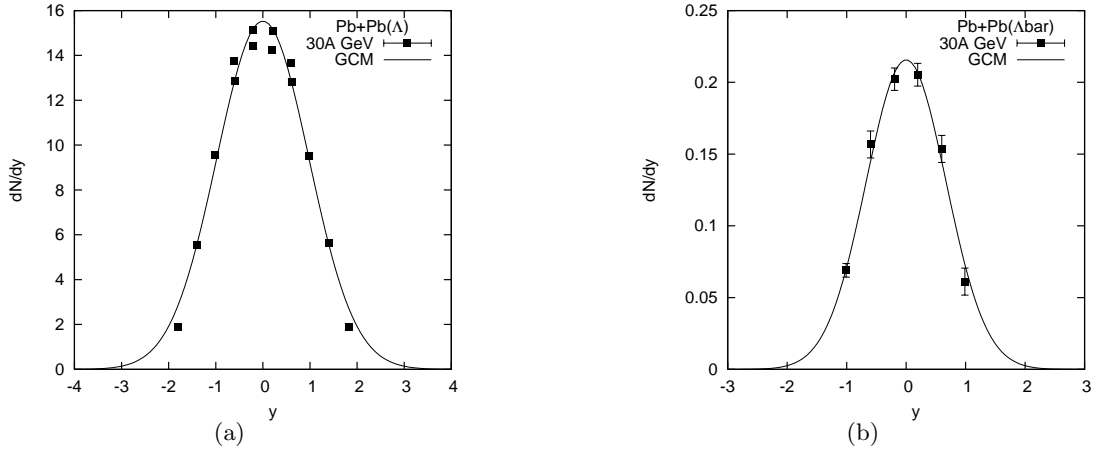


Figure 3: Rapidity spectra for Λ and $\Lambda\bar{\Lambda}$ produced in Pb+Pb collisions at 30A GeV for $\beta=0$. The different experimental points are taken from [10] and the parameter values are taken from Table 2. The solid curve provide the GCM-based results.

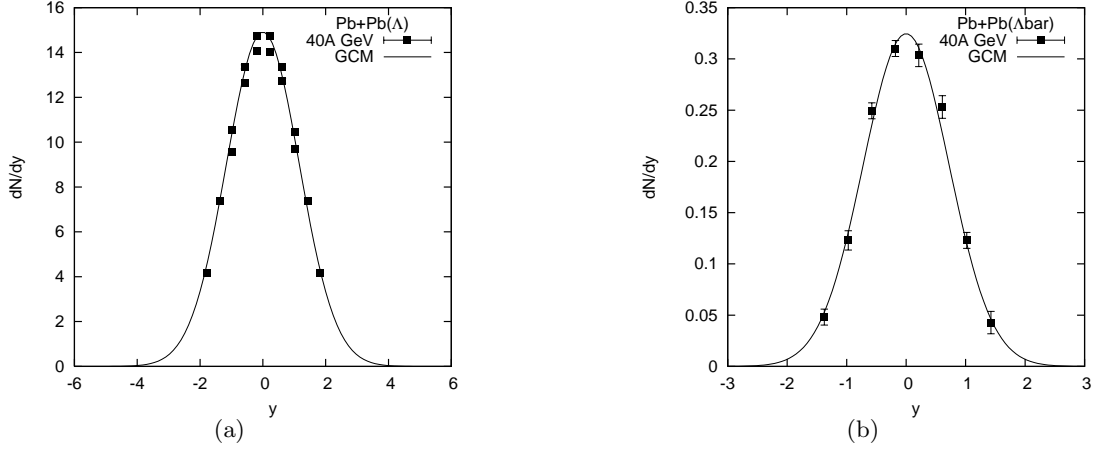


Figure 4: Plot of $\frac{dN}{dy}$ vs. y for Λ and $\bar{\Lambda}$ produced in Pb+Pb collisions at 40A GeV for $\beta=0$. The different experimental points are taken from [10] and the parameter values are taken from Table 2. The solid curve provide the GCM-based results.

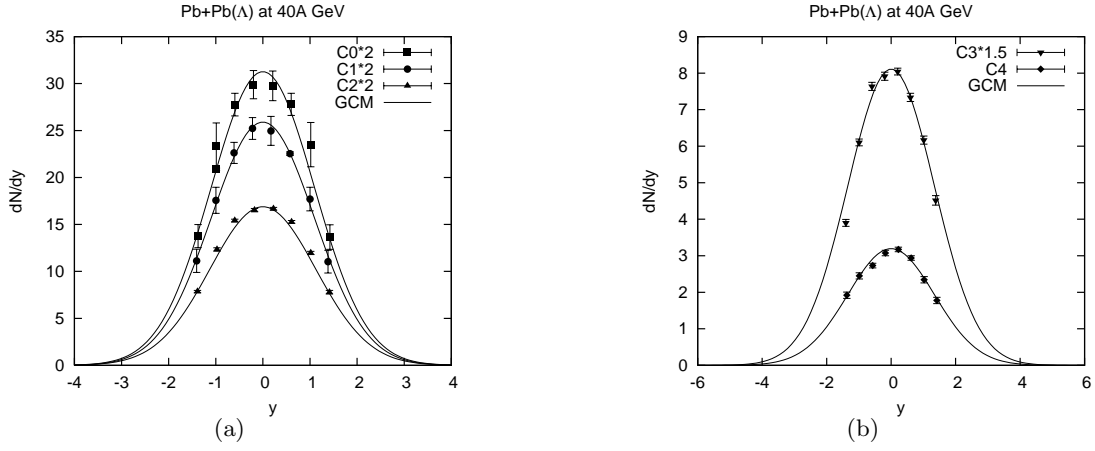


Figure 5: The rapidity spectra of Λ for Pb+Pb collisions at 40A GeV for the five different centrality bins C0-C4 for $\beta=0$. The experimental points are taken from [11] and the parameter values are taken from Table 3. The solid curves provide the GCM-based results.

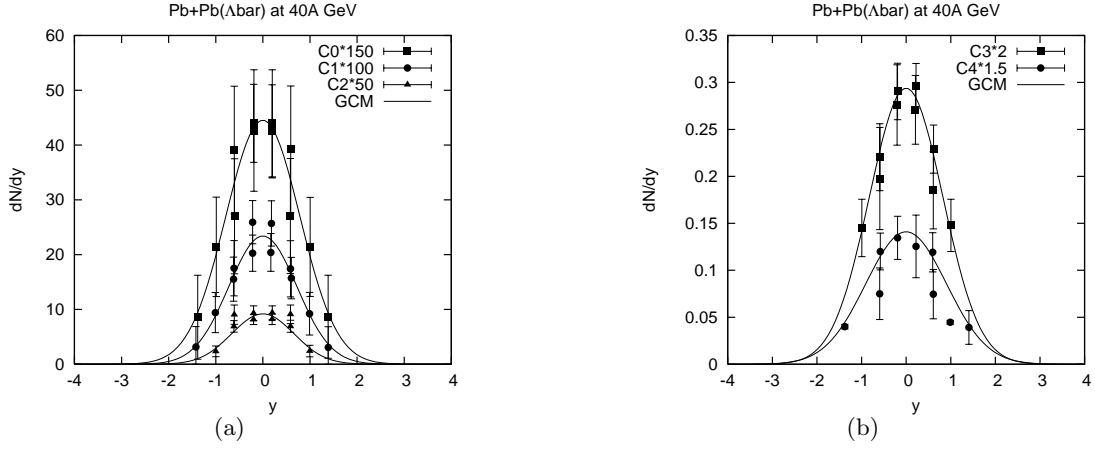


Figure 6: The rapidity spectra of Λ bar for Pb+Pb collisions at 40A GeV for the five different centrality bins C0-C4 for $\beta=0$. The experimental points are taken from [11] and the parameter values are taken from Table 4. The solid curves provide the GCM-based results.

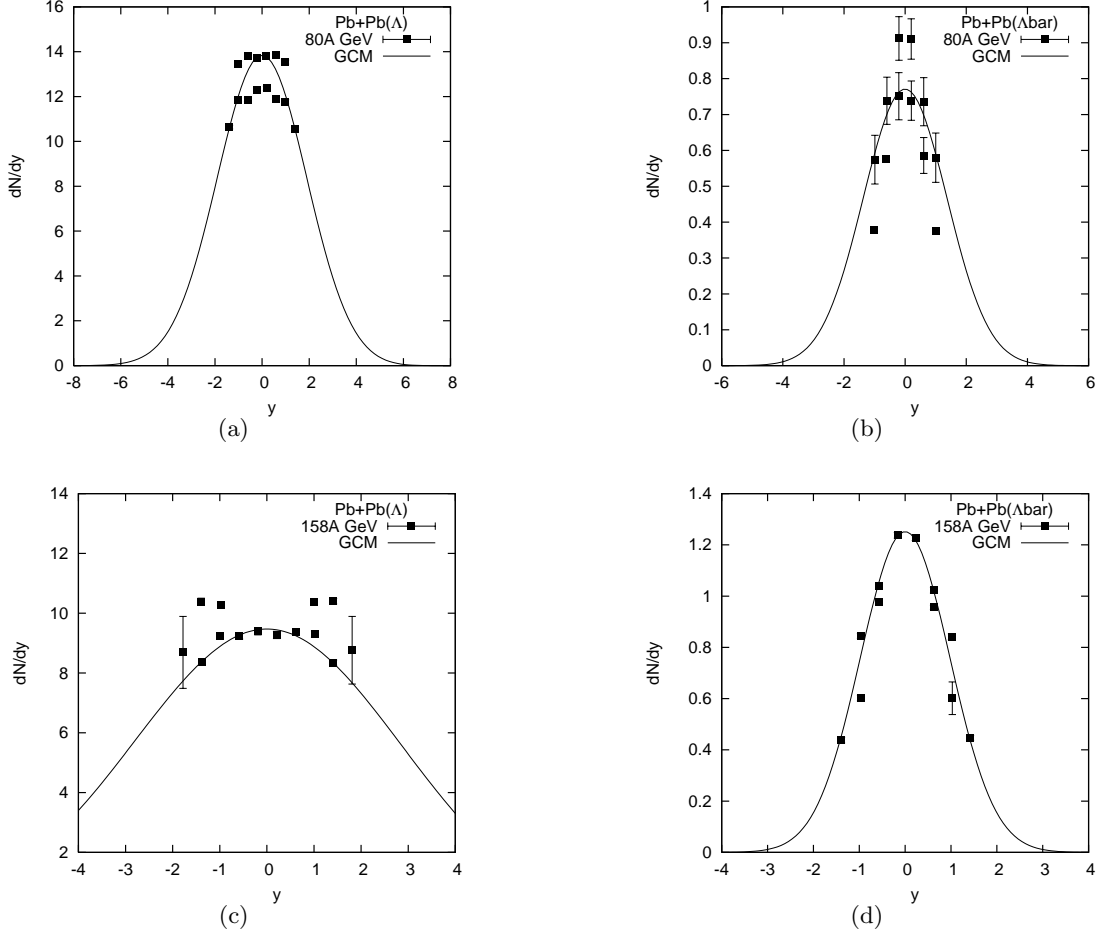


Figure 7: Rapidity spectra for Λ and $\bar{\Lambda}$ produced in Pb+Pb collisions at 80A GeV [Fig.6(a) and Fig.6(b)] and 158A GeV [Fig.6(c) and Fig.6(d)] for $\beta=0$. The different experimental points are taken from [10] and the parameter values are taken from Table 5. The solid curve provide the GCM-based results.

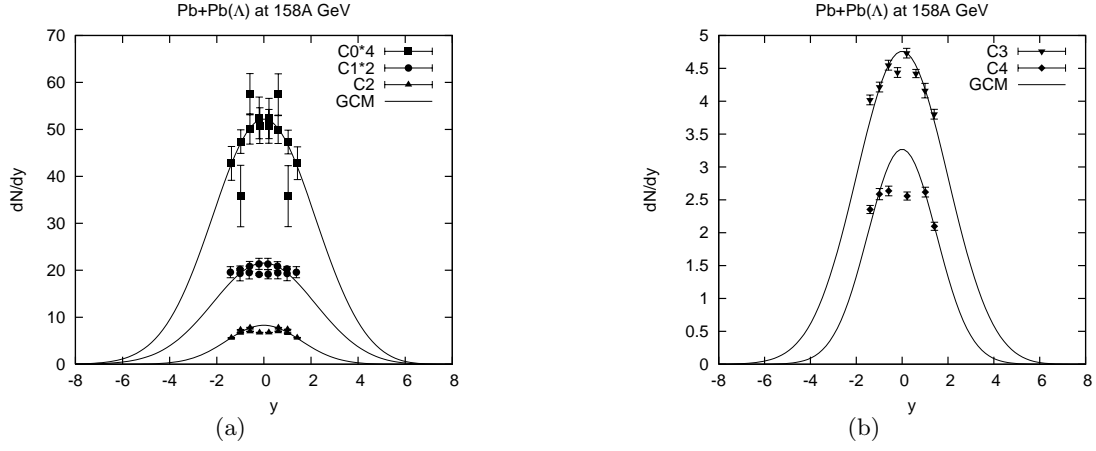


Figure 8: The rapidity spectra of Λ for Pb+Pb collisions at 158A GeV for the five different centrality bins C0-C4 for $\beta=0$. The experimental points are taken from [11] and the parameter values are taken from Table 6. The solid curves provide the GCM-based results.

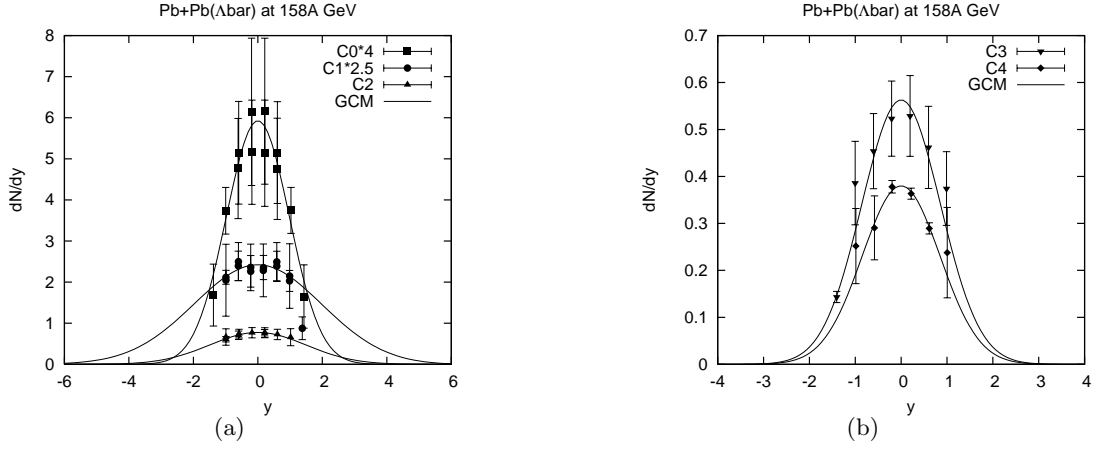


Figure 9: The rapidity spectra of Λ bar for Pb+Pb collisions at 158A GeV for the five different centrality bins C0-C4 for $\beta=0$. The experimental points are taken from [11] and the parameter values are taken from Table 7. The solid curves provide the GCM-based results.

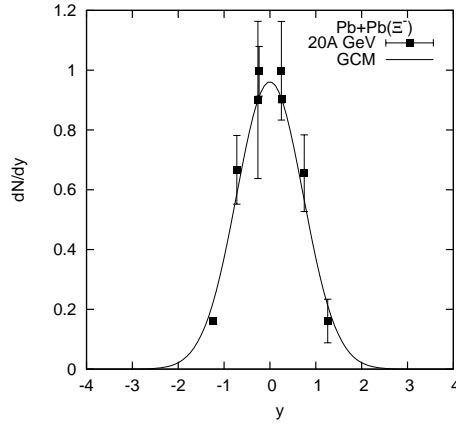


Figure 10: Rapidity spectra for Ξ^- produced in Pb+Pb collisions at 20A GeV for $\beta=0$. The different experimental points are taken from [10] and the parameter values are taken from Table 8. The solid curve provide the GCM-based results.

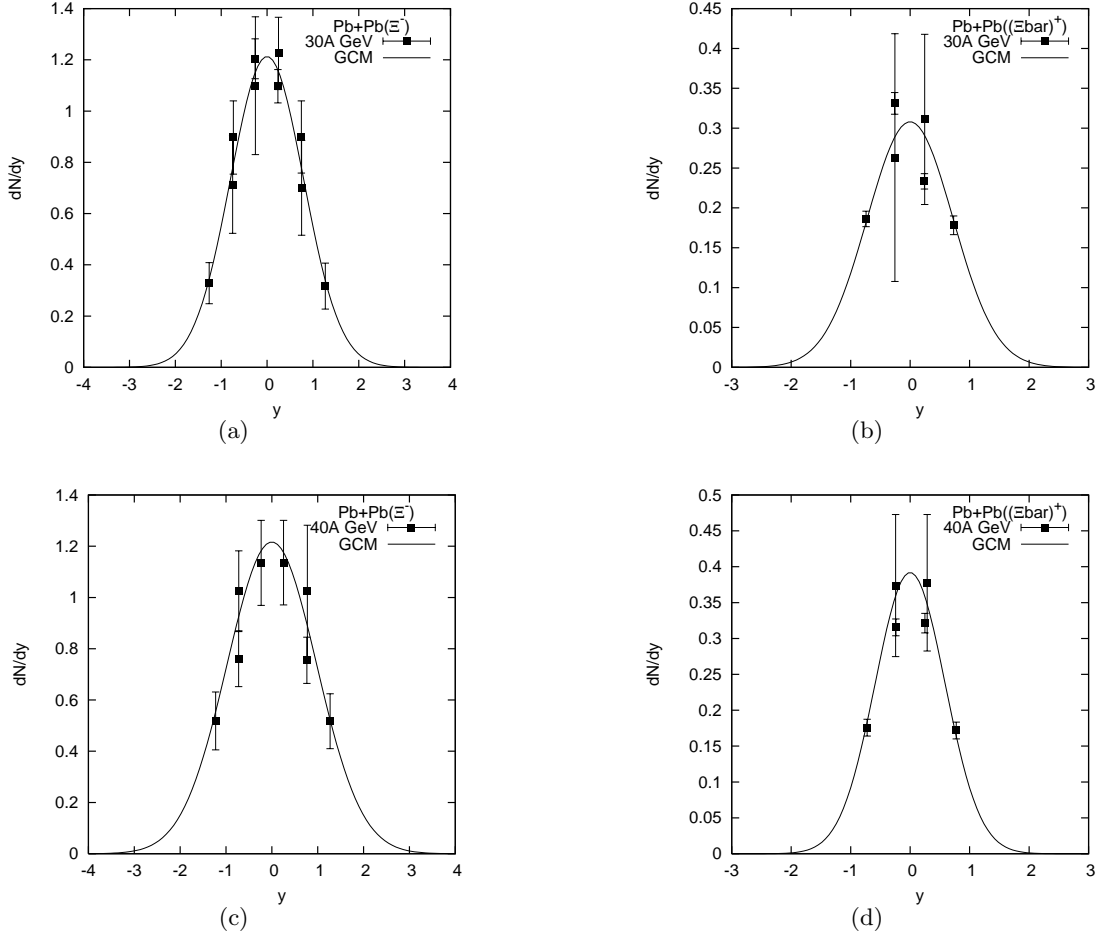


Figure 11: Plot of $\frac{dN}{dy}$ vs. y for Ξ^- and Ξbar^+ produced in Pb+Pb collisions at 30A GeV [Fig.12(a) and Fig.12(b)] and 40A GeV [Fig.12(c) and Fig.12(d)] for $\beta=0$. The different experimental points are taken from [10] and the parameter values are taken from Table 8. The solid curve provide the GCM-based results.

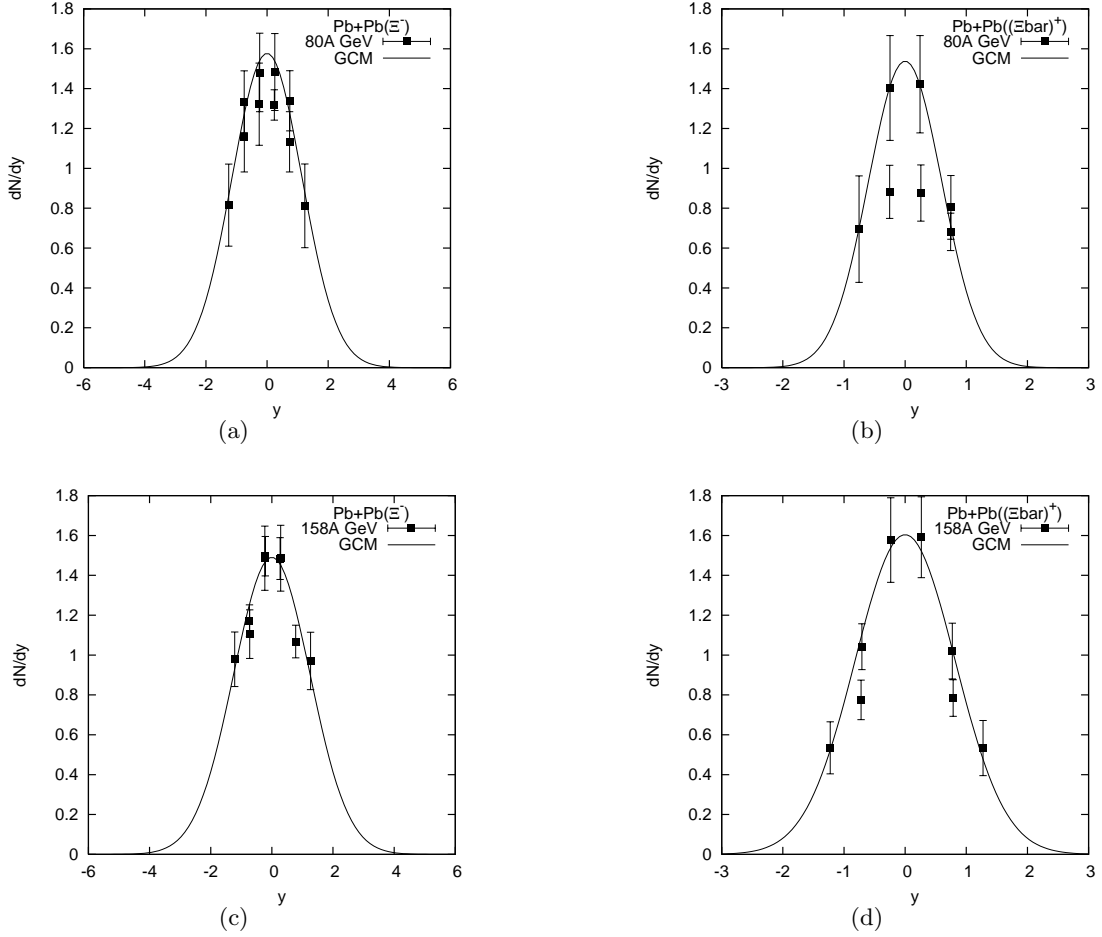


Figure 12: Rapidity spectra for Ξ^- and $\Xi^{\bar{+}}$ produced in Pb+Pb collisions at 80A GeV [Fig.11(a) and Fig.11(b)] and 158A GeV [Fig.11(c) and Fig.11(d)] for $\beta=0$. The different experimental points are taken from [10] and the parameter values are taken from Table 9. The solid curve provide the GCM-based results.

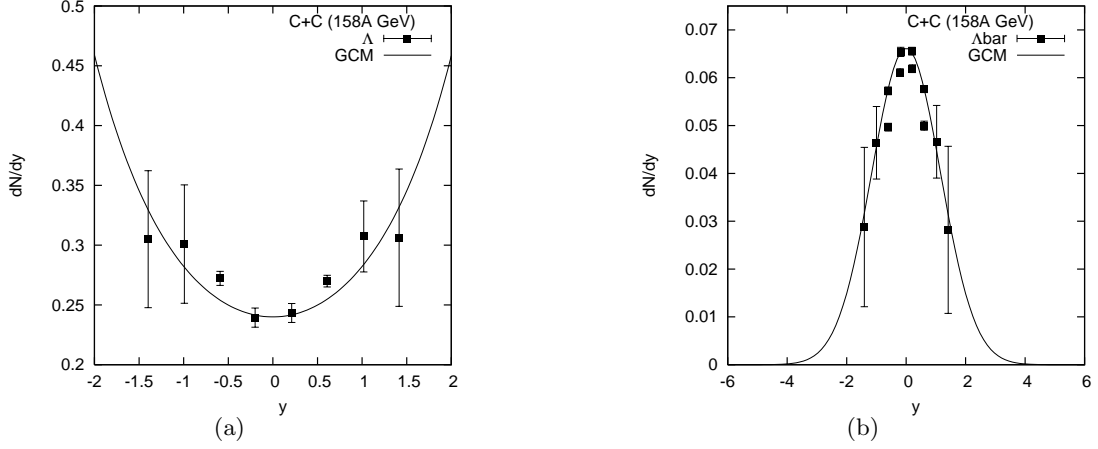


Figure 13: The rapidity spectra of Λ and $\bar{\Lambda}$ for near central C+C collisions at 158A GeV for $\beta=0$. The experimental points are taken from [11] and the parameter values are taken from Table 10. The solid curve provide the GCM-based results.

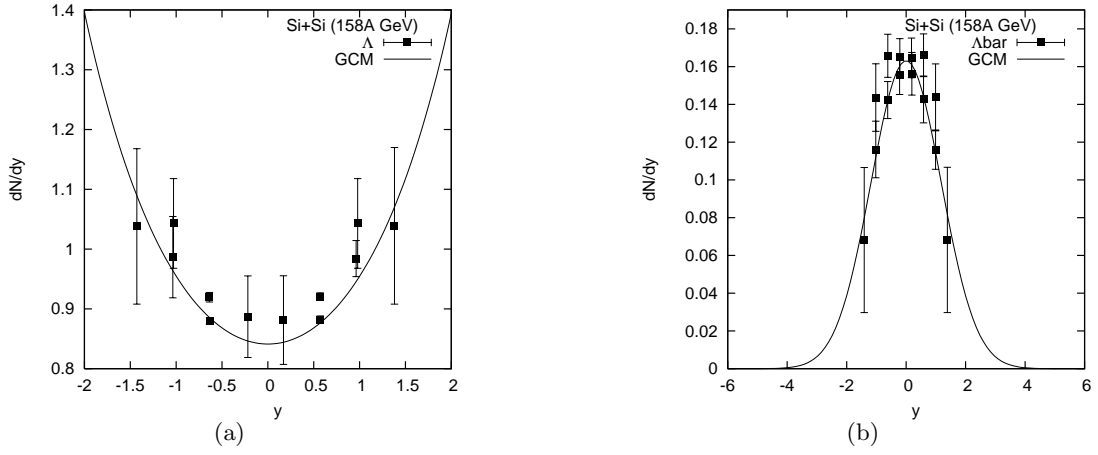


Figure 14: The rapidity spectra of Λ and $\bar{\Lambda}$ for near central Si+Si collisions at 158A GeV for $\beta=0$. The experimental points are taken from [11] and the parameter values are taken from Table 10. The solid curve provide the GCM-based results.